

A Neuro-Inspired Hierarchical Reinforcement Learning for Motor Control

Pei Zhang, Zhaobo Hua, Jinliang Ding, *Senior Member, IEEE*

Abstract—Designing controllers to achieve natural motion capabilities for multi-joint robots is a significant challenge. However, animals in nature are naturally with basic motor abilities and can master various complex motor skills through acquired learning. On the basis of analyzing the mechanism of the central motor system in mammals, we propose a neuro-inspired hierarchical reinforcement learning algorithm that enables robots to learn rich motor skills and apply them to complex task environments without relying on external data. We first design a skills network similar to the cerebellum by utilizing the selection mechanism of voluntary movements in the basal ganglia and the regulatory ability of the cerebellum to regulate movement. Subsequently, by imitating the structure of advanced centers in the motion system, we propose a high-level policy to generate different skill combinations, thereby enabling the robot to acquire natural motor abilities. We conduct experiments on 4 types of robots and 22 task environments, and the results show that the proposed method can enable different types of robots to achieve flexible motion skills. Overall, our research provides a promising framework for the design of robotic neural motor controllers.

Index Terms—Basal ganglia, motion control, multi-joint robot, neuroscience, reinforcement learning (RL).

I. INTRODUCTION

ENABLING robots to have universal, flexible, and adaptive motion capabilities in complex environments has always been a significant challenge, and reinforcement learning emerges as an important and feasible way to address this challenge [1]. Through carefully designed reward functions, robots can acquire flexible motion abilities [2] [3]. However, traditional reinforcement learning methods usually focus on learning specific tasks, resulting in limited generalization ability of motion controllers and insufficient flexibility in the generated actions. Once the task changes, the controller needs to be retrained.

In fields such as computational vision, researchers advocate the use of large-scale data to obtain universal models, thereby enabling intelligent agents to quickly adapt to downstream tasks [4]. Combining this pre-training method with hierarchical reinforcement learning [5], recent studies have made progress

in designing smart robot motion controllers. Unsupervised reinforcement learning methods encourage robots to collect different experiences and evolve diverse skills through intrinsic rewards [6], enabling them to quickly adapt to downstream tasks. Under unsupervised conditions, the exploration ability of agents is greatly improved, but they will develop skills unrelated to downstream tasks. Goal space conditioned approaches balance exploration efficiency and universality by establishing a specialized goal space during pre-training, but the design of the goal space requires a large amount of expert knowledge [7]. On the contrary, data-driven methods enable robots to generate highly realistic actions by learning from a large amount of collected data. For example, adversarial skill embedding (ASE) is a promising method that uses unstructured motion clips to train a low-level latent variable model [8], allowing robots to generate actions similar to the dataset. But obtaining and maintaining such datasets can be a costly task.

Although these methods have made significant progress in motion control, they still cannot achieve animal like motor abilities. In nature, mammals are born with some basic natural motor abilities (such as balance, crawling, etc.). Through learning, they will acquire more complex skills to solve tasks in various scenarios. The natural motor ability of animals mainly comes from their central motor system [9], which has a natural three-level structure [10]. The highest level includes the association area of neocortex in the brain and the basal ganglia, responsible for generating complex motor strategies. The middle level is composed of the motor cortex and cerebellum, which participate in the formation of orderly control signals. The lowest level is composed of the brain stem and spinal cord, responsible for executing actions. In this hierarchical structure, the central motor system exhibits autonomy, and even without signals from higher levels, lower systems can generate diverse behaviors. Many animals can still retain basic motor ability even with most of their brain tissue removed [11] [12]. Based on this autonomy, some studies have taken a central pattern generator based on spinal cord loop reflection mode as a motion controller [13] [14]. However, the motion trajectory generated by this method is relatively monotonous, as more complex movements require the participation of higher levels control mechanisms, and low-level control mechanisms can be repeatedly called upon by the higher levels, i.e., the repeatability. In addition, higher-level institutions are often responsible for abstracting information [15], and their signals have a longer duration [16] [17]. This also reflects the state and time abstraction.

In this article, we combine the mechanisms and principles of

This work was supported in part by the National Key R&D Plan Project under Grant 2022YFB3304700, the National Natural Science Foundation of China under Grant 61988101, the 111 Project 2.0 under Grant B08015, and the Liaoning Province Central Leading Local Science and Technology Development Special Project under Grant 2022JH6/100100055. (Corresponding author: Jinliang Ding)

P. Zhang and Z. Hua, and J. Ding are with the State Key Laboratory of Synthetical Automation for Process Industries, Northeastern University, Shenyang 110819, China (email: pei.zhang088@outlook.com; Bobby_1752635630@outlook.com; jlding@mail.neu.edu.cn).

Parts of the figure were drawn by using pictures from Servier Medical Art. Servier Medical Art by Servier is licensed under a Creative Commons Attribution 3.0 Unported License (<https://creativecommons.org/licenses/by/3.0/>).

the central motor system to propose a neuro-inspired hierarchical reinforcement learning algorithm (NIHRL) for intelligent motion behavior control of multi-joint robots. Through this algorithm, we can obtain flexible motion controllers that enable robots to generate natural motion capabilities and solve various complex downstream tasks without relying on any external data. In the experimental section, we demonstrate the application of the proposed algorithm on four different robots and enable them to perform at least five intricate tasks. The experimental results show that our approach has better performance in complex task environments compared to existing state-of-the-art (SOTA) algorithms. The flexible motion ability of robots also proves the effectiveness of central motion system mechanisms in robot control. This study makes the following contributions to the field of reinforcement learning and robot control:

1) On the basis of analyzing the mechanism of the central motor system, we propose a two-level neuro-inspired hierarchical reinforcement learning algorithm. The cerebellar network can generate different robust behavioral patterns according to various motor skills, while the cortical network can generate skill signals that repeatedly call upon the cerebellar network, endowing robots with complex motor abilities in various challenging environments.

2) Through the analysis of the mechanisms of the basal ganglia, we propose a skill activity function and validate its rationality by simulating Parkinson's disease and Huntington's disease. This function provides a reasonable tool to quantify the activity of motor skills.

3) Based on the basic motor regulation function of the cerebellum, we design a fusion reward mechanism that combines motor ability and skill exploration. This mechanism enables us to obtain low-level skill policy similar to the cerebellum.

4) In order to encode discrete skills during pre-training, we design an encoding method that helps to spread a small number of discrete skills into dense continuous spaces, thereby promoting skill expression.

The rest of this article is organized as follows. Section II and Section III present relevant research progresses and preliminaries. Section IV presents the structure of the central motor system and the proposed the NIHRL algorithm. The results of the simulation experiments are presented in Section V. Finally, the conclusion is summarized in Section VI.

II. RELATED WORK

Recent work in the field of pre-training RL can be divided into three groups based on the methods used: unsupervised reinforcement learning, goal space conditioned learning, and data-driven learning.

A. Unsupervised Reinforcement Learning

Unsupervised reinforcement learning enables agents to collect different experiences and self learn useful skills in the environment through intrinsic rewards. According to the composition of intrinsic rewards, these studies can be divided into three types: data-based, skill-based, and knowledge-based.

1) Data-based methods mainly explore data diversity by maximizing data coverage. Hazan et al. [18] employed the conditional gradient method, also known as the Frank Wolfe algorithm, to propose an effective algorithm named MaxEnt for optimizing objectives defined intrinsically. Liu & Abbeel [19] presented the Active Pre-Training algorithm (APT), which conducts environmental exploration by maximizing a non-parametric entropy calculated within an abstract representation space. Yarats et al. [20] introduced Proto-RL, a self-supervised framework that unites representation learning with exploration using prototypical representations. These representations are designed to generalize across various tasks while also accelerating subsequent exploration for more efficient task-specific training.

2) The skill-based approach primarily achieves skill diversity by maximizing mutual information between states s and skills z . Achiam et al. [21] presented VALOR, a method derived from contextual learning. In VALOR, the policy encodes contextual information from a random distribution into trajectories, and the decoder subsequently reconstructs the contextual data from the full trajectories. Park et al. [22] introduced LSD, a method that incentivizes the agent to explore a broader spectrum of diverse and dynamic skills with extended reach. Their study tackled the problem commonly observed in MI (mutual information) methods [21], where a preference for static skills is evident over dynamic ones. Eysenbach et al. [23] introduced DIAYN, which optimizes information theory objectives through maximum entropy policy to achieve skill learning, providing a solution for solving exploration challenges and improving data efficiency in reinforcement learning. Liu & Abbeel [24] introduced APS by reinterpreting and merging variational successor features [25] with non-parametric entropy maximization [19]. APS overcomes the constraints of current unsupervised RL methods based on mutual information maximization and entropy maximization, effectively amalgamating the strengths of both approaches.

3) The knowledge-based method increases the agent's understanding of the world by maximizing prediction errors. Pathak et al. [26] presented ICM, a method that leverages curiosity as an intrinsic reward signal, enabling the agent to investigate its surroundings and acquire valuable skills. Burda et al. [27] introduced RND, a novel approach that effectively merges intrinsic and extrinsic rewards, leading to notable advancements in challenging exploration tasks within Atari games.

B. Goal Space Conditioned Learning

Although unsupervised learning can accelerate the adaptation speed of intelligent agents to downstream tasks, it is difficult to balance skill universality and sampling efficiency. The Goal space method is a compromise approach. By designing appropriate skill spaces, a balance can be achieved between them. Gehring et al. [7] alleviated the need for prior knowledge by proposing a hierarchical skill learning framework that acquires skills of varying complexity in an unsupervised manner. Shi et al. [28] proposed a novel reinforcement learning based method that consists of a foot trajectory generator.

This generator continuously optimizes given tasks to provide different motion priors to guide policy learning. Campos et al. [29] pointed out that the operations discovered by the existing algorithms have low coverage of the state space and proposed an alternative approach to information-theoretic skill discovery. The disadvantage of these methods is that the target space is difficult to design, requiring extensive expert knowledge and repeated experiments.

C. Data-Driven Learning

The above two methods have shown good results in low dimensional space. However, for complex robots with higher degrees of freedom, relying solely on unsupervised or target space design makes it difficult to achieve natural motion effects. Learning motor skills from data is an effective means to solve the motion control of high degree of freedom multi-joint robots. On the basis of the Inverted Pendulum Model (IPM), Kwon and Hodgins [30] proposed the Momentum Mapped IPM (MMPM), which allows for various behaviors such as walking, running, and a series of gymnastics movements. Xu and Karamouzas [31] introduced their GAN-like approach; the proposed method can separately train multiple motor control strategies to mimic different behaviors. Peng et al. [32] demonstrated that RL techniques can be utilized to acquire robust control policies that can replicate various motion clips. However, the aforementioned methods based on tracking and imitation often encounter difficulties when facing large-scale and diverse action datasets, requiring action planners to combine and select different skills. Park et al. [33] presented a network-based algorithm that learns control policies from unorganized, minimally-labeled human motion data. Peng et al. [34] adopted a two-level hierarchical control framework, which aimed to learn various environment-aware locomotion skills with a limited amount of prior knowledge. Although the above two methods can learn the target policy from limited prior knowledge, they still need to learn from scratch. Combining techniques from adversarial imitation learning and unsupervised reinforcement learning, Peng et al. [8] presented a large-scale data-driven framework ASE for learning versatile and reusable skill embeddings for physically simulated characters. This method does not require learning from scratch and can embed various skills. However, the difficulty of such methods lies in the difficulty and high cost of obtaining and maintaining motion capture data.

III. PRELIMINARY

A. Reinforcement Learning

Reinforcement learning is an optimization method based on Markov Decision Processes (MDP). At each time step t , the environment provides a state s_t to a policy π , then the policy generates an action $a_t \sim \pi(a_t|s_t)$ based on the state [1]. The environment executes a_t and generates the next state $s_{t+1} \sim p(s_{t+1}|s_t, a_t)$ and a reward $r_t = r(s_t, a_t, s_{t+1})$. From the state s_t at time t until the termination state, the sum of all discounted rewards is called the return G_t , and the function

of the return is given by the following equation, where γ is the discount factor between 0 and 1.

$$G_t = \sum_{k=0}^{\infty} \gamma^k r_{t+k}. \quad (1)$$

The value $V_{\pi}(s_t)$ of state s_t is defined as the mathematic expectation $\mathbb{E}_{\pi}[G_t|S_t = s_t]$ of the return G_t from that state to the termination state. Reinforcement learning seeks the optimal policy by maximizing the return expectation starting from the initial state s_0 . The time horizon of the reinforcement learning process in this article is finite. Within a certain time step T , the policy will generate a finite trajectory $\tau = \langle s_0, a_0, s_1, r_0, \dots, s_{T-1}, a_{T-1}, s_T, r_{T-1} \rangle$, the goal of RL is to find the optimal policy π^* to maximize the following return function

$$J(\pi) = \mathbb{E}_{\tau \sim \pi} \left[\sum_{t=0}^{T-1} \gamma^t r_t \right]. \quad (2)$$

B. Hierarchical Reinforcement Learning and Pre-training

Hierarchical Reinforcement learning (HRL) uses a hierarchical structure to decompose complex tasks into simple subtasks, thereby achieving the goal of simplifying problems [5]. HRL is an optimization method defined in the Semi-Markov Decision Process (SMDP) process, which introduces the concept of time in the basic MDP process.

Taking two-layer reinforcement learning as an example, the high-level policy selects a subtask (skill) z_t as its action, the action lasts for k time steps, and the goal of this policy is to select the appropriate sequence of subtasks to complete the solution of the main task [35]. The low-level policy selects the primary action a_t based on the state s_t and subtask z , maximizing the internal reward r_t^l to complete the subtask. For the low-level policy, the $r_t^l = r(s_t, a_t, s_{t+1}, z)$, and each step will generate experience $e_t^l = \langle s_t, a_t, r_t^l, s_{t+1} \rangle$, during the execution of each subtask, trajectory $\tau^l = \langle s_t, a_t, r_t^l, s_{t+1}, \dots, s_{t+k-1}, a_{t+k-1}, r_{t+k-1}^l, s_{t+k} \rangle$ will be generated. For the high-level policy, $r_t^h = \sum_{i=t}^{t+k-1} [\gamma^{i-t} r(s_i, a_i, s_{i+1}, z)]$, and every k -step will generate experience $e_t^h = \langle s_t, z_t, r_t^h, s_{t+k} \rangle$, the trajectory $\tau^h = \langle s_0, z_0, r_0^h, s_{0+k}, \dots, s_{T-k}, z_{T-k}, r_{T-k}^h, s_T \rangle$ will be generated during the time horizon T . The goal of HRL is to find the optimal low-level policy π_l^* and high-level policy π_h^* to maximize the following return functions:

$$J(\pi_l) = \mathbb{E}_{\tau^l \sim \pi_l} \left[\sum_{i=t}^{t+k-1} \gamma^{i-t} r_i^l \right], \quad (3)$$

$$J(\pi_h) = \mathbb{E}_{\tau^h \sim \pi_h} \left[\sum_{i=0}^{T/k-1} \gamma_h^i r_{i \cdot k}^h \right], \quad (4)$$

where $\gamma_h = \gamma^k$.

Pre-training aims to use various means to obtain a good exploratory low-level policy, in order to promote the learning of downstream tasks. When using pre-training mode, the low-level and high-level policies are trained independently. The above process will be decoupled into two separate MDP

processes. We first optimize the low-level policy in a pre-training environment. After obtaining the low-level policy, we fix its parameters to collect data during the execution of the high-level policy, thereby optimizing the high-level policy.

C. Mutual Information for Skill Exploration

Mutual information is a commonly used reward method in skill-based unsupervised reinforcement learning algorithms [36] [23]. The core idea of this method is to maximize the mutual information between the state s generated by policy π and skill z , thereby encouraging agents to correspond different skills to different states. Mutual information rewards can be expressed as follows

$$\begin{aligned} I(s; z|\pi) &= I(z; s|\pi) \\ &= \mathcal{H}(z) - \mathcal{H}(z|s, \pi_\theta) \\ &= -\mathbb{E}_{p(z)} [\log p(z)] + \mathbb{E}_{p(z)} \mathbb{E}_{p(s|\pi, z)} [\log p(z|s, \pi)]. \end{aligned} \quad (5)$$

Calculating $p(z|s, \pi)$ during training is a tricky task. Reference [37] introduces $q(z|s)$ as a variational approximation for this value. From $\mathcal{H}(p) \leq \mathcal{H}(p, q)$, the following equation can be obtained

$$\begin{aligned} I(s; z|\pi) &\geq -\mathbb{E}_{p(z)} [\log p(z)] + \mathbb{E}_{p(z)} \mathbb{E}_{p(s|\pi, z)} [\log q(z|s)]. \end{aligned} \quad (6)$$

In order to make the variational approximation $q(z|s)$ closer to the actual distribution $p(z|s, \pi)$ during the training process, we parameterize q into a discriminator network $q_\varphi(z|s)$. During the training process, it is necessary to continuously optimize the parameter φ to make its estimated value $q_\varphi(z|s)$ closer to the real skill z . In this work, we encode discrete skill z into continuous skill z^c . Therefore, for a certain skill, the variational approximation target can be represented by

$$\min_{\varphi} L(\varphi) = -\frac{1}{B} \sum_{j=1}^B \sum_{i=0}^{C-1} T_o(z_j)_i \log[q_\varphi(z|s_j)_i], \quad (7)$$

where $T_o(z)$ represents the one-hot encoding of the discrete skill z , B represents the size of the sampled batch, and C represents the number of types of discrete skills.

IV. PROPOSED APPROACH

Our research focuses on seamlessly integrating central motor system with reinforcement learning to design intelligent universal robot motion controllers. In this section, we first analyze the operating mechanism of the central motor system. We then propose the NIHRL algorithm and explain how to train cerebellar and cortical networks in steps. Finally, we summarize the NIHRL algorithm using its pseudo code.

A. Central Motor System Abstract Structure

The hierarchical mechanism of the mammalian central motor system can be described in Fig. 1, with different control hierarchy levels distinguished by varying colors. The blue boxes represent the highest level, the yellow boxes represent the middle level, and the brown boxes represent the lowest level. In addition, the gray dashed boxes are used in the figure

to represent the sensing areas related to motion control, while the elliptical shapes represent some brain structures related to information transmission.

The highest level mechanism (blue box) consists of a portion of the cerebral cortex and basal ganglia. According to the Brodmann partition [38], this mechanism mainly includes the posterior parietal cortex (areas 5 and 7) and prefrontal cortex, basal ganglia, as well as the supplementary motor area (SMA) and premotor cortex (PMA) located in area 6. Firstly, areas 5 and 7 of the parietal cortex serve as the input parts of the highest level structure, responsible for processing proprioceptive information from the somatosensory cortex (areas 1, 2, and 3) and external information from the visual cortex (areas 17, 18, and 19), respectively. The prefrontal cortex is connected to the posterior parietal cortex and is responsible for further processing information from the parietal lobe. Subsequently, the basal ganglia processes information from the prefrontal cortex, and through its internal regulatory processes, transmits the results to the oral part of the thalamic ventral lateral nucleus (VLo), and then to the cortical area 6, especially SMA. Then SMA and PMA participate in motion planning together [39] and send control signals to the next level control mechanism.

The middle level mechanism (yellow box) is mainly composed of the pons, cerebellum, and the primary motor cortex located in cortical area 4. The proprioceptive information from the somatosensory cortex and the control signals from the cortical area 6 pass through the pontine nucleus in the pons, transmit to the cerebellum, and finally project to the primary motor cortex through the caudal part of the thalamic ventral lateral nucleus (VLc). During this process, the cerebellum controls the sequential contraction of muscles, and patients with cerebellar injury will be unable to maintain balance and exercise accuracy. The primary motor cortex is mainly responsible for compiling decision information from the thalamus into more basic control signals composed of force and direction [9].

Ultimately, the primary motor cortex transmits these basic control signals to the lowest level executing mechanisms (brown box), including the brain stem and spinal cord, thereby mobilizing muscle cells to enable animals to complete complex movements (as shown on the right side of Fig. 1).

The basal ganglia plays a complex regulatory role in the process of motor decision-making at the highest level. Researches have shown that the complex structures within the basal ganglia form direct and indirect pathways [40] [41] [42] [43]. They are respectively responsible for enhancing and inhibiting voluntary movement, which is regulated by the inhibitory neurotransmitter gamma-aminobutyric acid (GABA) and the excitatory neurotransmitter glutamate (Glu). The mechanism of the regulatory process is shown in Fig. 1. The direct pathway originates from the striatum, passes through the internal segment of the globus pallidus (GPi) and the substantia nigra pars reticulata (SNr), and finally reaches SMA via VLo. Specifically, the prefrontal cortex releases Glu, which excites the striatum and leads to increased GABA release, thereby inhibiting GPi neurons and liberating cells in VLo from inhibition. VLo releases a large amount of Glu, enhancing

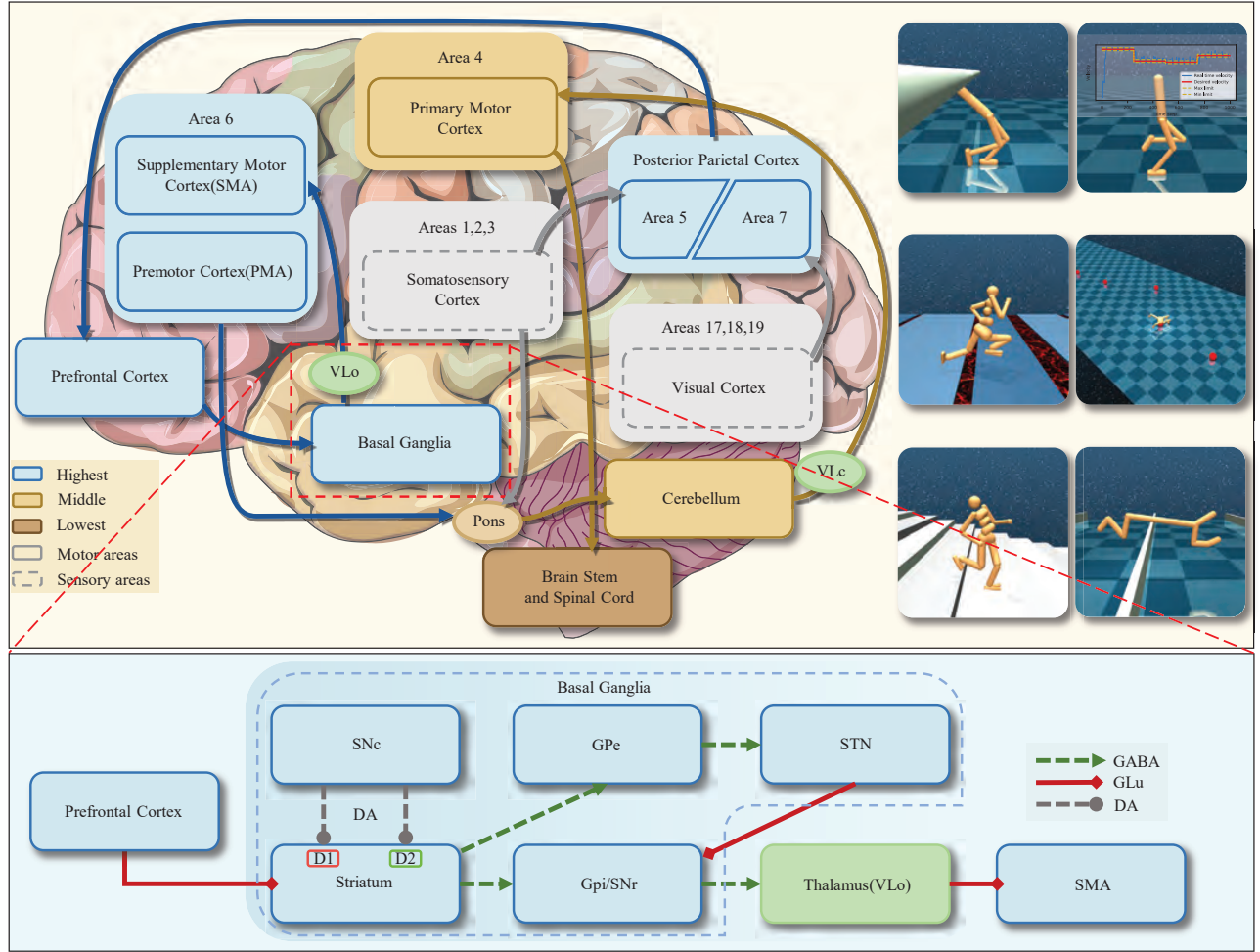


Fig. 1. The central motor system mechanism, with three colors representing different levels of the motor system, and sensory and motor regions distinguished by dashed and solid lines. This mechanism can be applied to the motion control of various robots and enable them to complete complex tasks. The enlarged portion of the red dashed line displays the physiological mechanism of the basic ganglia.

the activity of SMA. On the contrary, the indirect pathway extends from the striatum to the external segment of the globus pallidus (GPe), then passes through the subthalamic nucleus (STN) to GPi, and finally from VLo to SMA. The striatum inhibits cells in GPe and weakens its inhibitory effect on STN. Therefore, STN releases a large amount of Glu to activate neurons in GPi, which naturally inhibits VLo neurons and weakens cortical activity. In addition, the substantia nigra pars compacta (SNc) exerts opposite effects on the D1 and D2 receptors in the striatum by releasing dopamine (DA). The activation of D1 receptors enhances the direct pathway, while the activation of D2 receptors inhibits the indirect pathway. Therefore, DA overall enhances the activity of the cortex. We mainly study how to model and apply this mechanism in an end-to-end manner to robotics motion control. Although the internal mechanisms of the basal ganglia are complex, their ultimate impact on motion mainly depends on the Glu concentration projected from the thalamus to the cortex. Based on this characteristic, we design a skill activity function (Section IV.C), which enables the controller to mimic the regulatory effect of the basal ganglia on motor willingness.

B. Neuro-Inspired Hierarchical Reinforcement Learning Algorithm

Based on the results of the hierarchical mechanism of the central motor system, we propose a NIHRL algorithm for robotics motion control, and use the Mujoco physics engine [44] to build a robot motion simulation environment. The overall structure of the algorithm is shown in Fig. 2. The execution mechanism of the simulation engine is used to replace the lowest level nervous systems, such as the brain stem, spinal cord, and muscles, while its sensor mechanism is used to simulate the input units of the nervous system for additional information, such as somatosensory information and vision. On the contrary, the middle and the highest levels mechanisms of the central motor system correspond to the low-level and high-level policies of the algorithm, respectively. Through the pre-training process and the task-training process, we can obtain the cerebellar network (low-level policy) and cortical network (high-level policy). With the coordination and cooperation of the two networks, robots can exhibit exceptional mobility. The cortical network generates skill information z for each k time step. For each time step,

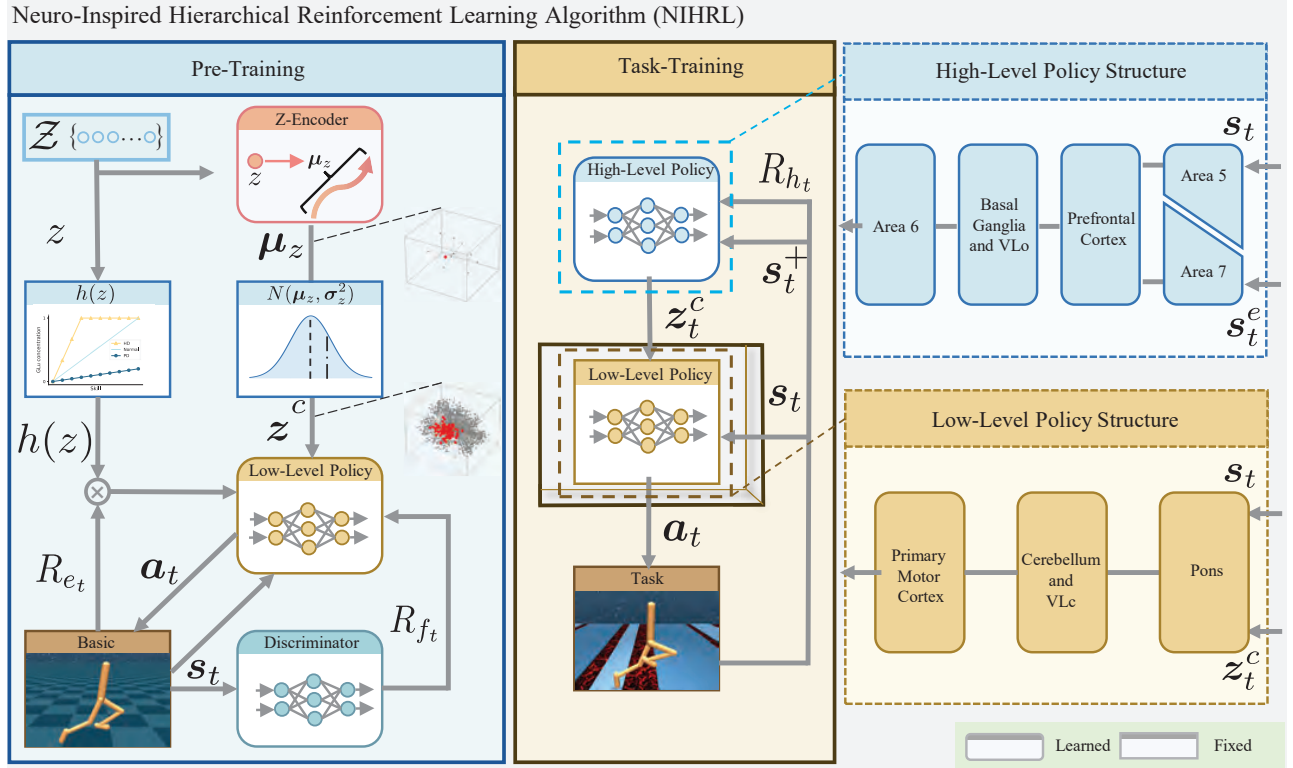


Fig. 2. The NIHRL algorithm is divided into two parts: in the pre-training phase, a cerebellar network (low-policy) is obtained, which is responsible for receiving signals from the basal ganglia and adjusting the robot's willingness to move and posture. Through task-training, a cortical network (high-policy) is obtained, which is responsible for processing external environmental information and generating skill signals suitable for task solving.

the cerebellar network receives robot states s and z to generate appropriate primary actions a .

The pre-training stage is conducted in the basic environment, which only includes the robot itself, and its observation space is composed of proprioception s_t . The cerebellar network is a parameterized neural network $\pi_{\theta}(a|s, z^c)$, and we use fusion reward R_a to train the parameters. The internal architecture of the neural network corresponds to the middle level mechanism of central motor system, including the pons, cerebellum, and primary motor cortex. The input includes proprioceptive information s_t and skill information z_t^c from cortical area 6, while the output is a temporal action signal a_t . The output signal is transmitted to the simulation environment to drive the robot's motion. During the pre-training stage, the skill activity function $h(z)$ designed by the basal ganglia motor regulation mechanism is responsible for evaluating the activity of skills and assigning activity as a weight for the motor reward R_e . This reward and the mutual information reward R_f calculated by the discriminator together form the fusion reward R_a . When the training reward converges, we obtain the cerebellar network as a fixed low-level policy for subsequent training.

The task-training phase is conducted in the task environment, which not only include robots but also include additional environmental information (such as obstacles, targets, etc.). We use sparse rewards R_h to train the cortical network, which is modeled as a parameterized neural network $\psi_{\omega}(z^c|s, s^e)$.

At this point, the pre-trained cerebellar network is fixed and serves as the lower-level actuator of the cortical network. The internal architecture of the cortical network corresponds to the highest level mechanism of central motor system. The proprioceptive information s_t and external environmental information s_t^e are processed separately by the input terminals of the two heads, corresponding to the functions of the two partitions of the central motor system posterior parietal cortex. Subsequently, the prefrontal cortex fuses information and obtains skill decision-making instructions through the dimensionality reduction and selection of the basal ganglia. This instruction is further processed through the motor cortex area 6 to obtain a skill vector z_t^c that can be input into the cerebellar network. The output action execution cycle of the cortical network is longer, and the dimension is lower, which also reflects the temporal and state abstraction of the nervous system. During task-training, the obtained policy is evaluated every certain period of time to measure the motion ability brought to the robot by the algorithm.

C. Learning the Cerebellar Network

The cerebellar network $\pi_{\theta}(a|s, z^c)$ needs to have the ability to regulate basic movements and balance, as well as the ability to flexibly respond to high-level skill information. Skills can regulate the activity level of cerebellar network output motion and generate different robot motion postures.

In order to learn the regulation of basic movements, we design a basic motor reward R_e .

$$R_e = w_v v_x - w_c u^2 + w_f I[s \notin \bar{s}], \quad (8)$$

where w_v is the the weight of torso velocity, w_f is the weight of balance ability, and w_c is the weight of energy consumption. $I[\cdot]$ is the indicator function, \bar{s} is the invalid state after a fall, and u is the control signal generated by the cerebellar network.

On this basis, the high-level skills need to be used as input to the neural network to regulate the motion functions. Combining the approaches in reference [21] [23], we contextually encode the discrete skill z from a uniformly distributed $p(z) = U(0, C-1)$ to form a continuous skill z_c as a potential skill for pre-training. Z-encoder is a layer of trainable neural network, parameterized as E_ξ , which encodes discrete skills into d_{μ_z} -dimensional continuous vectors, i.e., $\mu_z = E_\xi(z)$.

Next, in order to enhance robustness, we randomly process continuous vectors μ_z by $z_c \sim N(\mu_z, \sigma_z^2)$, and constrain the resulting vectors to the range of $(-1, 1)$. These vectors z_c form a part of the skill space \mathcal{Z}^c , while the other part of \mathcal{Z}^c is composed of the remaining random vectors z_r^c that are not sampled during the pre-training period. To ensure the diversity of encoding skills, we update E_ξ by maximizing the L2 norm between continuous skill vectors, which is called the Skill Diversity (SD) objective.

$$\min_{\xi} L(\xi) = - \sum_{k=0}^{C-2} \sum_{l=k+1}^{C-1} \|\hat{\mu}_{z_k} - \hat{\mu}_{z_l}\|_2, \quad (9)$$

where C is the number of discrete skills, and $\hat{\mu}_z = \frac{\tanh(\mu_z)}{\|\mu_z\|_2}$.

To simulate the regulatory effect of basal ganglia on motor activity, we design a skill activity function, linking skills with different Glu concentrations, and using it as the weight of the basic motor reward R_e .

$$h(z) = \min \left(\frac{b_{glu}}{C-1} z, 1 \right), \quad (10)$$

where b_{glu} is the activity influence factor of the function.

In order to generate different robot postures for different skills, we use mutual information as part of the pre-training reward, namely $R_f = -\log p(z) + \log q_\varphi(z|s)$. For the state s of high-dimensional robots, we preprocess it using ϕ function.

Taking into account the above steps, we can obtain a fusion reward function as follows

$$R_{a_t} = \beta [-\log p(z) \log q_\varphi(z|\phi(s_{t+1}))] + (1 - \beta) h(z) R_{e_t}, \quad (11)$$

where β is the proportion of reward.

And the optimization objective of the pre-training can be described using Equation (12). To ensure the stability of the training process, we adopt the SAC algorithm [45] to train the network. This algorithm can robustly solve control problems in continuous observation space and continuous action space without requiring extensive hyperparameter adjustment.

$$\max_{\theta, \xi} \mathbb{E}_{p(z)} \mathbb{E}_{p(\tau|\pi_\theta, E_\xi(z))} \left[\sum_{t=0}^{T-1} \gamma^t R_{a_t} \right]. \quad (12)$$

D. Learning the Cortical Network

After obtaining the cerebellar network $\pi_{\theta^*}(a|s, z^c)$, the high-dimensional continuous skill space \mathcal{Z}^c can be used to learn the cortical network $\psi_\omega(z^c|s, s^e)$. In order to maintain the consistency of the reward function in different tasks, the task environment rewards R_{h_t} as sparse rewards, and robots only receive positive rewards when completing a specified goal. Therefore, in this environment, robots need to have strong exploration ability to complete tasks.

According to the characteristics of the central motor system, the high-level policy has strict temporal abstraction, which means switching skill actions z_{c_t} every k time steps, while the low-level policy generates different basic actions a_t each time step. This temporal abstraction can lead to a decrease in the training efficiency of the cortical network, as only T/k transitions can be obtained within the T time step. Therefore, we adopt a step conditioned critical structure as described in [7] [46]. By using this architecture, we can obtain $T - (k - 1)$ transformed data within T time steps to increase the number of samples and ensure training efficiency under the constraints of time abstraction.

The optimization algorithm for the cortical network parameter ω still adopts SAC. However, due to the use of step-conditioned critic, some improvements need to be made to the value function $Q(s, s^e, z^c)$ of the SAC algorithm and its optimization objectives. To simplify calculations, both proprioception and additional environmental inputs are recorded as s^+ . The improved Q function has added input $i = t \bmod k (0 \leq i < k)$ to record the number of executed steps for advanced actions. The calculation method of the action value function Q is shown in Equation (13), and the calculation method of the entropy value function V is given in Equation (14).

$$Q(s_t^+, z_t^c, i) = \left(\sum_{j=0}^{k-i-1} \gamma^j R_{h_{t+j}} \right) + \gamma^{k-i} V(s_{t+k-i}^+). \quad (13)$$

$$V(s_t^+) = \mathbb{E}_{z_t^c \sim \psi} [Q(s_t^+, z_t^c, 0) - \alpha \log \psi(z_t^c | s_t^+)]. \quad (14)$$

By parameterizing the Q function using a neural network, denoted as $Q_v(s_t^+, z_t^c, i)$, one can update the parameters v by minimizing the Bellman residual using experiential data. The optimization objective is shown in Equation (15).

$$\min_v J(v) = \mathbb{E}_{(s_t^+, \dots, s_{t+k-1}^+, z_t^c, i) \sim \mathcal{B}} \left[\frac{1}{2} \left(Q_v(s_t^+, z_t^c, i) - G' \right)^2 \right], \quad (15)$$

where $G' = \sum_{j=0}^{k-i-1} (\gamma^j R_{h_{t+j}}) + \gamma^{k-i} V(s_{t+k-i}^+)$. And the optimization target for the cortical network parameters ω is provided in Equation (16).

$$\min_{\omega} J(\omega) = \mathbb{E}_{s_t^+ \sim \mathcal{B}} [\mathbb{E}_{z_t^c \sim \psi_\omega} [\alpha \log \psi_\omega(z_t^c | s_t^+) - Q_v(s_t^+, z_t^c, 0)]] . \quad (16)$$

E. Training Algorithms

Algorithm 1 provides the pseudo code for the pre-training process. In the pseudo code, *done* represents the condition for the agent to enter an invalid state or complete a round. Once *done*=True, a new episode begins. The policy and Q function are updated using Algorithm 1 in the SAC algorithm.

Algorithm 1 Pre-training pseudo code

```

1: Input: maximum number of episodes  $N$ ; learning rate  $\lambda$ ;
   batch size  $B$ ; discrete skills number  $C$ ; number pf update
   episodes  $n$ ;
2: Output: optimal parameters  $\theta^*$  for low-level policy;
3: Init:  $\pi_\theta \leftarrow$  low-level policy;  $E_\xi \leftarrow$  Z-encoder;  $q_\phi \leftarrow$ 
   discriminator;  $Q_\rho \leftarrow$  Q-function;  $\mathcal{B} \leftarrow$  Buffer;
4: for  $i \leftarrow 1, N$  do
5:   Sample skill  $z \sim p(z) = U(0, C - 1)$ 
6:   Compute  $h(z)$  according to Equation (10)
7:    $done = \text{False}$ 
8:   for time-step  $t = 0, \dots, T - 1$  do
9:     Sample continues  $z_t^c \sim N(E_\xi(z), \sigma_z^2)$ 
10:    Sample action  $a_t \sim \pi_\theta(a_t | s_t, \tanh(z_t^c))$ 
11:     $s_{t+1}, R_{e_t}, done \sim p(s_{t+1}, s_t^e, a_t)$ 
12:    Compute  $R_{a_t}$  according to Equation (11)
13:    Store  $(s_t, s_{t+1}, a_t, z, R_{a_t})$  in  $\mathcal{B}$ 
14:     $s_t \leftarrow s_{t+1}$ 
15:    if  $done$  then
16:       $break$ 
17:    end if
18:  end for
19:  Update discriminator:
20:  for update-step  $u = 1, \dots, n$  do
21:     $b_B \leftarrow$  Sample batch of  $B$  transitions  $\{(s_j, z_j)\}_{j=1}^B$ 
    from  $\mathcal{B}$ 
22:    Update  $q_\phi$  according to Equation (7) using data from
     $b_B$ 
23:  end for
24:  Update z-encoder:
25:  for update-step  $u = 1, \dots, n$  do
26:    Get all skills  $(z_0, \dots, z_{C-1})$ 
27:    Compute unit vectors  $(\hat{\mu}_{z_0}, \dots, \hat{\mu}_{z_{C-1}})$  using  $E_\xi(z)$ 
28:    Update  $E_\xi$  according to Equation (9)
29:  end for
30:  Update low-level policy:
31:  for update-step  $u = 1, \dots, n$  do
32:    SAC-UPDATE  $E_\xi, \pi_\theta$  and  $Q_\rho$  according to Equation
    (12) using data from  $\mathcal{B}$ 
33:  end for
34: end for

```

Algorithm 2 provides the pseudo code for the task-training process. In the pseudo code, the parameters of the low-level policy are initialized by θ^* obtained from Algorithm 1.

V. EXPERIMENT

A. Experimental Setup

To test NIHRL, we use the Mujoco simulation engine [44] to design six challenging motion control environments for

Algorithm 2 Task-training pseudo code

```

1: Input: maximum number of episodes  $N$ ; learning rate  $\lambda$ ;
   batch size  $B$ ; number of update episodes  $n$ ; high action
   interval  $k$ ;
2: Output: optimal parameters  $\omega^*$  for high-level policy;
3: Init:  $\pi_{\theta^*} \leftarrow$  learned low-level policy;  $Q_v \leftarrow$  Q-function;
    $\mathcal{B} \leftarrow$  Buffer;
4: for  $i \leftarrow 1, N$  do
5:    $done = \text{False}$ 
6:   for time-step  $t = 0, \dots, T - 1$  do
7:     Compute  $i = (t \bmod k)$ 
8:     if  $i == 0$  then
9:       Sample high-action  $z_t^c \sim \psi_\omega(z_t^c | s_t, s_t^e)$ 
10:    end if
11:    Sample action  $a_t \sim \pi_{\theta^*}(a_t | s_t, z_t^c)$ 
12:     $s_{t+1}, s_{t+1}^e, R_{h_t}, done \sim p(s_{t+1}, s_{t+1}^e | s_t, s_t^e, a_t)$ 
13:    Store  $(s_t, s_{t+1}, s_t^e, s_{t+1}^e, z_t^c, R_{h_t}, i)$  in  $\mathcal{B}$ 
14:     $s_t, s_t^e \leftarrow s_{t+1}, s_{t+1}^e$ 
15:    if  $done$  then
16:       $break$ 
17:    end if
18:  end for
19:  SAC-UPDATE high-policy and high Q-function:
20:  for update-step  $u = 1, \dots, n$  do
21:    Update  $Q_v$  according to Equation (16) using data
    from  $\mathcal{B}$ 
22:    Update  $\psi_\omega$  according to Equation (17) using data
    from  $\mathcal{B}$ 
23:  end for
24: end for

```

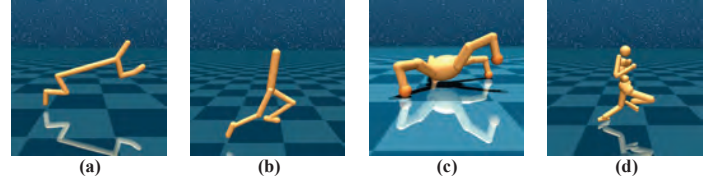


Fig. 3. Different types of robots in simulation environments. (a) “Cheetah”. (b) “Walker”. (c) “Quadruped”. (d) “Humanoid”.

four different types of robots, and conduct experiments in these environments. The types of robots are shown in Fig.3, including “Cheetah”, “Walker”, “Quadruped”, “Humanoid”. The first two types of robots are low degree of freedom robots in two-dimensional space, while the latter two are high degree of freedom robots in three-dimensional space.

The environments are divided into two types: basic environment and task environment. The basic environment is used to train and test the cerebellar network, while the task environment is used to train the cortical network and test the overall performance of algorithms. It should be pointed out that during the pre-training period, we preprocess the states of the “Quadruped” and “Humanoid” robots using the function ϕ to calculate the mutual information reward R_f . For “Quadruped”, we use the swing decomposition method [47] to calculate the rotation angles of x, y, and z from the global direction of the torso. In addition, we also calculate the

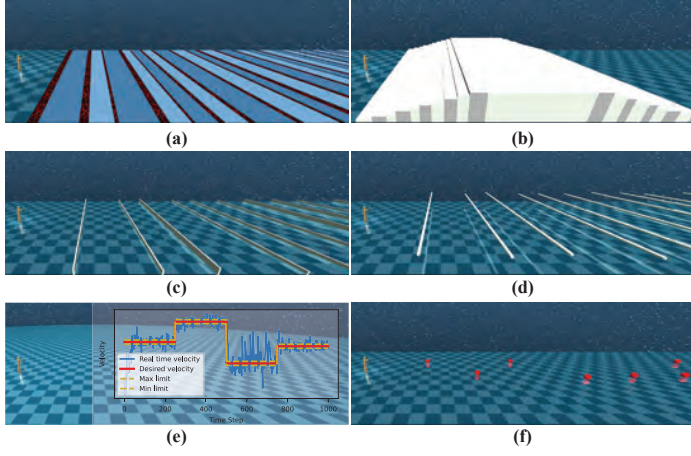


Fig. 4. Different task environments. (a) “Gaps”: The robot needs to constantly move forward and cross the magma, but once the robot comes into contact with the magma or falls, the task ends. (b) “Stairs”: The robot needs to cross the steps of ascent and descent. (c) “Hurdles”: The robot needs to adjust its posture to cross the hurdles. (d) “Limbo”: The robot needs to lower its center of gravity during movement to pass through the interceptor. (e) “V-track”: The robot needs to track four random expected speeds and maintain its own speed within a specified deviation range from the expected speed. (f) “Goals”: The robot needs to touch more target points within a limited time.

distances of the four toes relative to the torso in the x , y , and z directions and use the above information as the preprocessed state $\phi(s)$. As for “Humanoid”, we adopt a similar approach to the former, but replace the relative distances with the positions of the remaining parts of the robot relative to the pelvis in the x , y , and z directions.

The task environment mainly designed based on the Bisk suite [7]. The tasks “Gaps”, “Stairs”, “Hurdles”, and “Limbo” remain unchanged. However, “Cheetah” and “Quadruped” robots are added to these tasks. And we design two new tasks, “V-track” and “Goals”, all tasks are shown in Fig.4. The reward function R_h for all tasks is in discrete form. When the robot meets the target requirements, it will receive a reward value of +1, while when the robot enters an invalid state, it will receive a reward of -1 and the task will terminate. Under other conditions, the reward is 0. The hyperparameters used in the pre-training process are shown in Table I, while the hyperparameters used in the task-training process are shown in Table II.

We first design experiments to verify the rationality of the skill activity function. We then evaluate the motion regulation ability of the cerebellar network in four types of robots in the basic environment. By comparing and conducting ablation experiments on the NIHRL algorithm, we analyze its working principle, advantages, and characteristics.

B. Rationality Analysis of Activity Function

To verify the rationality of the proposed skill activity function (Equation (10)), we simulate the impact of basal ganglia abnormalities on motor function. Under the influence of different skill activity functions, we can obtain different cerebellar networks through pre-training. By testing the impact of cerebellar networks on robot motor ability, we can achieve the various symptoms of basal ganglia dysfunction. In the

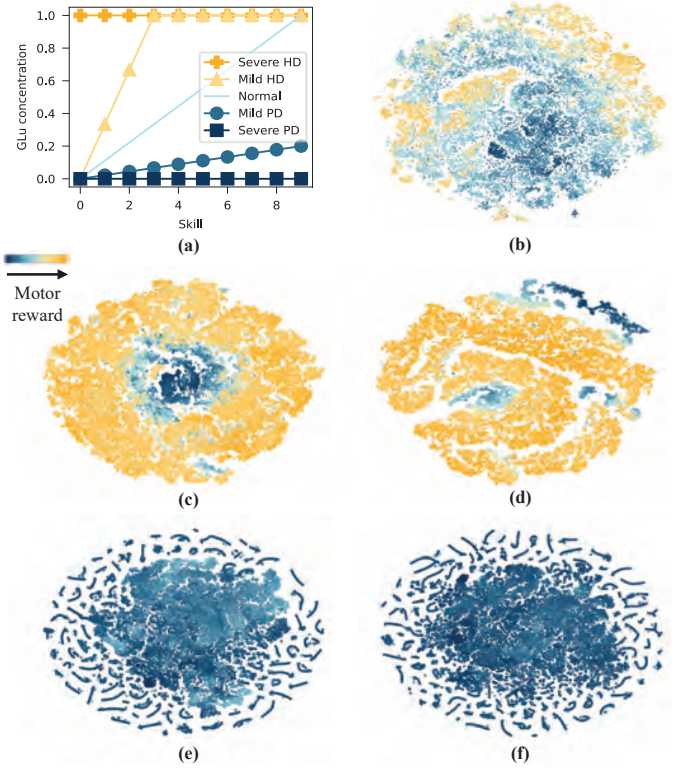


Fig. 5. Simulation results of the validation of the skill activity function (using the “Walker” robot as an example). (a) Skill activity function curves corresponding to different symptoms. The horizontal axis represents the discrete skill number, and the vertical axis represents Glu concentration. The t-SNE dimensionality reduction [48] scatter plot of state-skill pairs in different individuals: (b) Normal individuals. (c) Mild HD patients. (d) Severe HD patients. (e) Mild PD patients. (f) Severe PD patients.

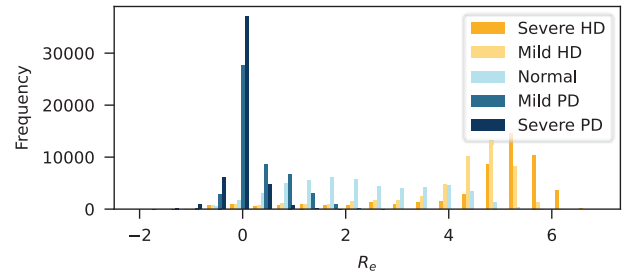


Fig. 6. The distribution frequency chart of basic motor rewards under different conditions.

experiment, C was taken as 10. The values of b_{glu} for several cases are shown in Table III.

The curves in Fig.5a represent the skill activity functions corresponding to individuals with severe Huntington’s disease (HD), individuals with mild HD, normal individuals, individuals with mild Parkinson’s disease (PD), and individuals with severe PD, from top to bottom. The scatter plots in Fig.5 show the distribution of basic motor reward values under the influence of different skill activity functions. The brighter the color, the stronger the robot’s willingness to move at this time. Each scatter corresponds to a state-skill pair (s_t, z_t^c) , and the scatter data are generated from 200 random skills

TABLE I
HYPER-PARAMETERS FOR PRE-TRAINING

Parameter	Value(Cheetah)	Value(Walker)	Value(Quadruped)	Value(Humanoid)
Total samples	$2 \cdot 10^7$	$2 \cdot 10^7$	$2 \cdot 10^7$	$2 \cdot 10^7$
Warmup samples	10^4	10^4	10^4	10^4
Batch size B	256	256	256	256
Buffer size	$3 \cdot 10^6$	$3 \cdot 10^6$	$3 \cdot 10^6$	$3 \cdot 10^6$
Horizon T	100	100	100	100
Parallel environments	10	10	10	10
Samples per update	500	500	500	500
Update numbers each time	50	50	50	50
Number of skills C	10	10	10	10
Latent skill dim d_{μ_z}	7	7	7	7
Torso velocity weight w_v	0.5	1.0	2.0	2.0
Balance ability weight w_f	0.0	0.0	0.1	0.1
Energy consumption weight w_c	0.1	0.1	0.1	0.1
Proportion of reward β	0.5	0.5	0.5	0.5
Activity influence factor b_{glu}	1.0	1.0	1.0	1.0
Std of skill coding σ_z	0.3	0.3	0.3	0.3
Optimizer	Adam	Adam	Adam	Adam
Learning rate λ_π	0.0003	0.0003	0.0003	0.0003
Learning rate λ_Q	0.0003	0.0003	0.0003	0.0003
Learning rate λ_q	0.0003	0.0003	0.0003	0.0003
Learning rate λ_α	0.0001	0.0001	0.0001	0.0001
Learning rate λ_E	0.00001	0.00001	0.00001	0.00001
Initial temperature α	0.1	0.1	0.1	0.1
Target entropy \bar{H}	$-\dim(\mathcal{A})=-6$	$-\dim(\mathcal{A})=-6$	$-\dim(\mathcal{A})=-12$	$-\dim(\mathcal{A})=-21$
Discount factor γ	0.99	0.99	0.99	0.99
Target network update factor $\bar{\tau}$	0.01	0.01	0.01	0.01

TABLE II
HYPER-PARAMETERS FOR TASK-TRAINING

Parameter	Value
Total samples	$1 \cdot 10^7$
Warmup samples	1000
Batch size B	256
Buffer size	$1 \cdot 10^6$
Horizon T	1000
Parallel environments	10
Samples per update	500
Update numbers each time	50
Optimizer	Adam
Learning rate λ_π	0.0003
Learning rate λ_Q	0.0003
Learning rate λ_α	0.0001
Initial temperature α	0.1
Target entropy \bar{H}	$-\dim(d_{\mu_z})=-7$
Discount factor γ	0.99
Target network update factor $\bar{\tau}$	0.005
Action interval k	3

TABLE III
ACTIVITY INFLUENCE FACTORS b_{glu} CORRESPONDING TO DIFFERENT DISEASES

b_{glu}	Sever HD	Mild HD	Normal	Mild PD	Sever PD
Value	$10.0(h(0) = 1.0)$	3.0	1.0	0.2	0.0

z^c . When the skill activity function is at a normal level, the activity function can correspond different skills to multiple Glu concentrations and the basal ganglia can regulate the thalamus to project different concentrations of Glu to SMA, resulting in different skills producing different motor activity (Fig.5b). However, for HD patients, genetic defects can lead to significant loss of striatal neurons [9] [49], and the damaged

indirect pathway blocks the inhibitory effect of basal ganglia on movement, leading to an increase in Glu concentration projected from the thalamus to the cortex. At this point, under the action of the activity function, most skills correspond to high Glu concentrations, thus HD patients may develop chorea and involuntary motor disorders. As shown in Fig.5c and Fig.5d, only a few skills can generate lower motor rewards. On the contrary, the degeneration of substantia nigra neurons in PD patients leads to insufficient dopamine release [50]. Correspondingly, the slope of the activity function curve is low, and all skills exhibit low activity. Therefore, PD patients may experience symptoms such as difficulty in autonomous movement. As shown in Fig.5e and Fig.5f, almost all skills can only cause slow motion in the robot, which is more pronounced under severe disease conditions. Finally, Fig.6 shows the distribution of basic motor rewards under different activity functions. In normal individuals, the distribution of motor rewards exhibits a relatively diverse pattern. On the contrary, the distribution of motor rewards in PD patients is concentrated on the left side, while the distribution in HD patients is concentrated on the right side. The simulation results show that the skill activity function can effectively simulate the working mechanism of the basal ganglia, proving the rationality of using $h(z)$ as a weight for motor rewards.

C. Evaluation of Cerebellar Network Motor Skills

The pre-training process continues until the fusion reward R_a converges. Fig.7 shows the mean and standard deviations of fusion rewards for different robots in each iteration. The means and variances are calculated over three learning sessions of 20 million samples each. The results show that all four robots achieved convergence of fusion rewards in pre-training.

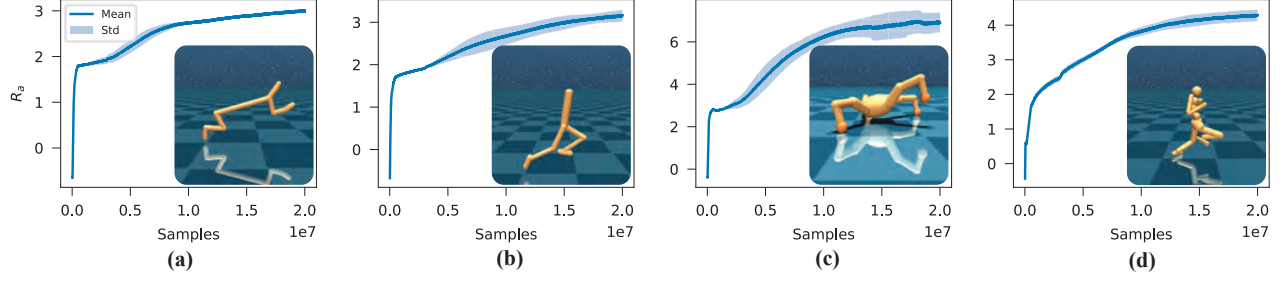


Fig. 7. The images of the fusion reward R_a of the four robots over time during the training process. The curve represents the average value obtained from three sets of random experiments, and the shaded portion represents the standard deviation. (a)“Cheetah”. (b)“Walker”. (c)“Quadraped”. (d)“Humanoid”.

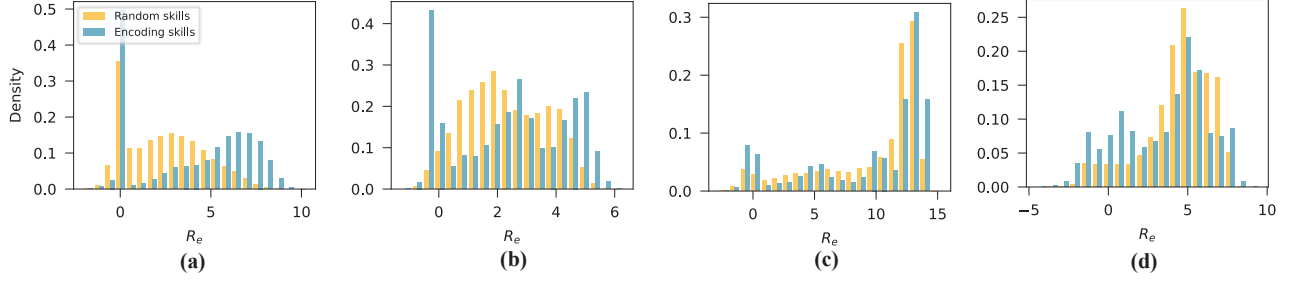


Fig. 8. The distributions of different basic motor rewards obtained by the cerebellar network under the influence of random skills from the skill space \mathcal{Z}^c and encoding skills \mathcal{z}^c from the z-encoder, respectively. Corresponding robots from left to right (a)“Cheetah”. (b)“Walker”. (c)“Quadraped”. (d)“Humanoid”.

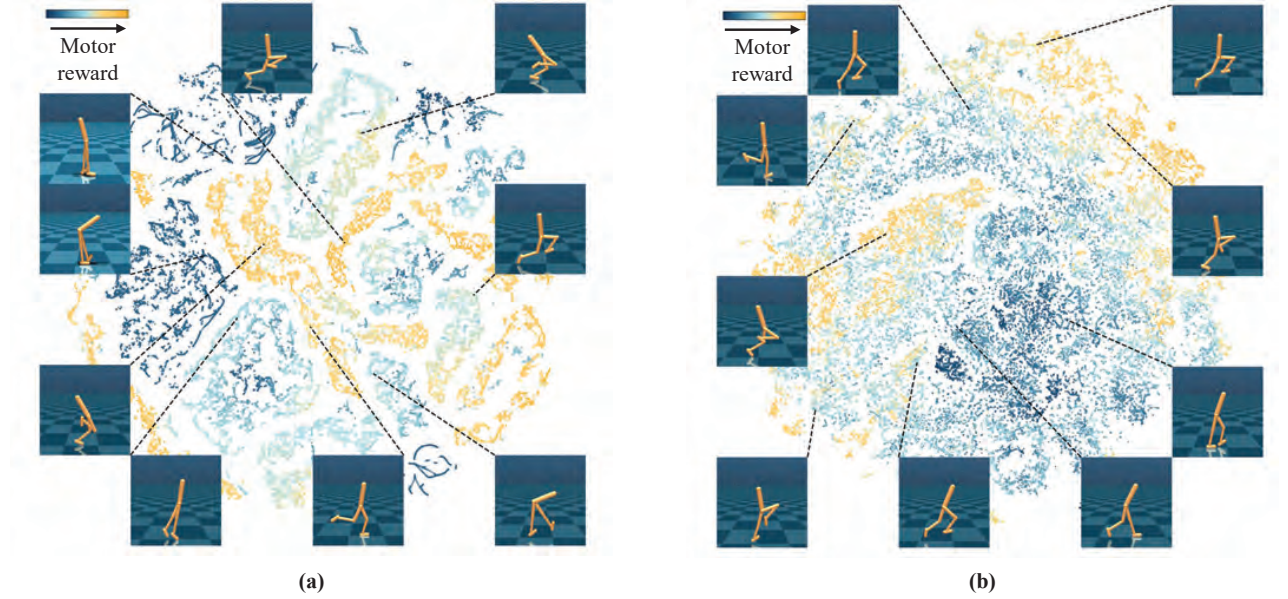


Fig. 9. (a) The state-skill pairs t-SNE scatter plot obtained by the cerebellar network of the “Walker” robot under the action of encoding skills \mathcal{z}^c . The black dashed lines in the figure connect the scattered points of the state-skill pairs and their corresponding robot joint state images. (b) The state-skill pairs t-SNE scatter plot obtained by the cerebellar network of the “Walker” robot under the action of random skills from the \mathcal{Z}^c .

Fig.8 shows the distributions of different basic motor rewards obtained by the trained cerebellar network under the influence of random skills from the skill space \mathcal{Z}^c and encoding skills \mathcal{z}^c from the z-encoder and the normal distribution $N(\mu_z, \sigma_z^2)$. It can be observed that the cerebellar network generates different motor activity under the influence of encoded different skills. Even if skills are randomly sampled from the high-dimensional skill space, this correspondence is basically not affected. This

owes to the randomness of skill encoding methods that provide robustness for the cerebellar network. In order to further explore the impact of different skills on robot motion ability, Fig.9 depicts the relationship between state-skill pairs and the joint state of the “Walker” robot. It can be seen that under the influence of different skills, the cerebellar network can not only maintain different levels of activity for the robot, but also affect the joint state of the robot. Comparing Fig.9a and Fig.9b,

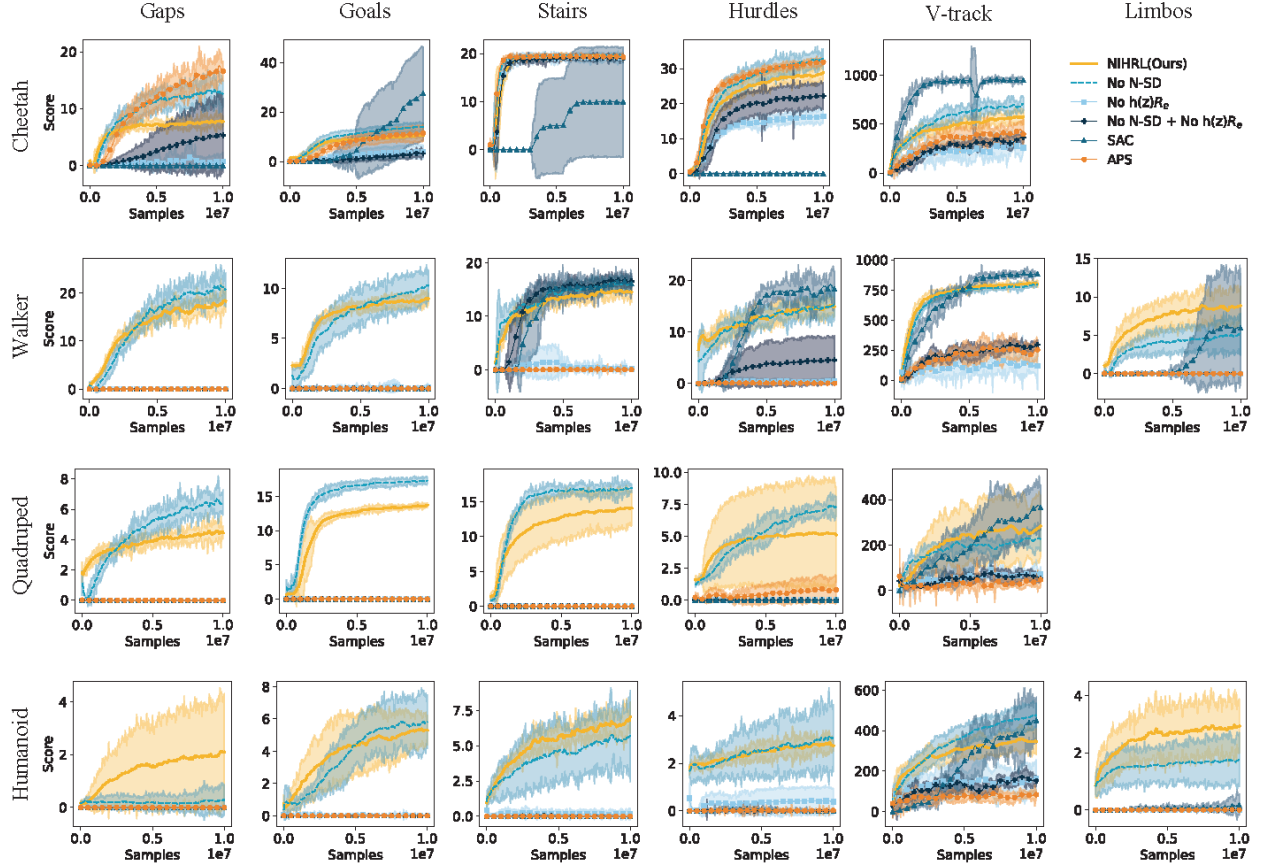


Fig. 10. Score curves of different algorithm training processes for four types of robots in 22 task environments. Including the APS algorithm, SAC algorithm and NIHL algorithm under normal conditions, and three missing conditions. For each algorithm and task, four pairs of random seeds were used for multiple experiments (two sets of random seeds formed four combinations during pre-training and task-training). The single score in each experiment is the average score of 50 test environments. The line represents the average score of four parallel experiments, while the shaded area represents the standard deviation.

it can be found that under the condition of random sampling skills, the cerebellar network can generate more diverse robot motion states.

D. Performance of NIHL Algorithm In Task Environments

In order to analyze the impact of various mechanisms on algorithm performance, we compare and explore the effects of different mechanisms during the pre-training stage on NIHL and the absence of skill activity function weighted motor reward (No $h(z)R_e$), absence of random distribution processing and skill diversity target (No N-SD), as well as the simultaneous absence of both (No N-SD + No $h(z)R_e$). In addition, we also compare the NIHL algorithm with the APS algorithm [24] to verify the effectiveness of the proposed pre-training method, where APS algorithm is an advanced skill-based unsupervised reinforcement learning algorithm. On the other hand, we also observe the effectiveness of directly using the SAC algorithm [45] to cope with complex tasks, in order to explore the advantages of hierarchical mechanisms.

Fig. 10 shows the score curves of four types of robots in various task environments under different circumstances. During the training process, the robots were evaluated 50 times for every 50,000 sample points sampled, and their average evaluation value was recorded as the score. The broken

line and shaded area represent the mean and variance of scores calculated in four experiments, with 10 million samples sampled in each experiment. Table IV presents these data in detail.

In the simplest “Cheetah” robot task environment, the models obtained under three missing conditions show comparable performance to the NIHL algorithm. But as the difficulty of robot control increases, the “No $h(z)R_e$ ” model cannot continue to produce meaningful results. This proves that the weighting mechanism of skill activity function on basic motor rewards plays a crucial role in the learning of robot motion skills. The “No N-SD” model performs similarly to NIHL in different task environments, and even slightly better than NIHL in low dimensional robot environments, but in the most complex “Humanoid” environment, the lack of diversity targets can lead to robots being unable to complete tasks that span gaps. This situation indicates that the skill diversity target and random distribution can enable robots with more joints to perform better in complex environments. In addition, the APS algorithm and the SAC algorithm only demonstrate control effectiveness in some tasks of the two types of planar robots, but the NIHL algorithm show robust control performance in all robot tasks. This proves the effectiveness of introducing the central motor system mechanism into the pre-training process

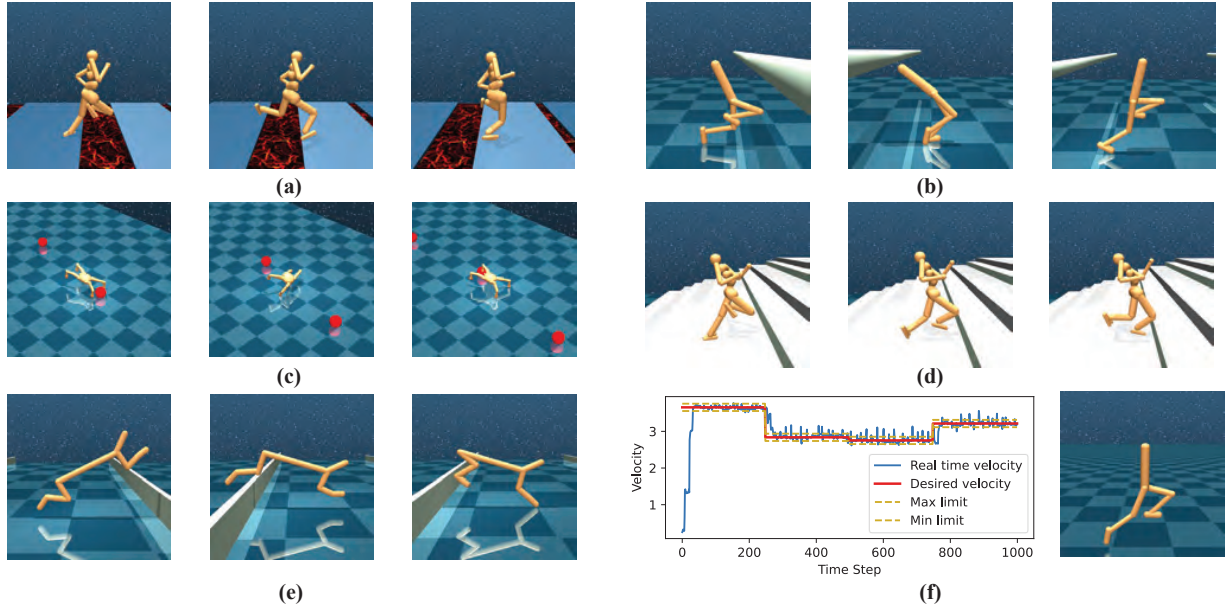


Fig. 11. The control performance of NIHRL algorithm in different robot task environments. (a) “Humanoid” robot in the “Gaps” task environment. (b) “Walker” robot in the “Limbo” task environment. (c) “Quadruped” robot in the “Goals” task environment. (d) “Humanoid” robot in the “Stairs” task environment. (e) “Humanoid” robot in the “Hurdles” task environment. (f) “Walker” robot in the “V-track” task environment. (g) “Walker” robot in the “V-track” task environment.

of reinforcement learning, and proves that the hierarchical mechanism of the nervous system can significantly improve the motion ability of robots.

After training, we can obtain cortical networks corresponding to different robots and tasks. By using the control circuit shown in Fig. 2 and connecting the cortical network and cerebellar network in series, the robot can be manipulated to complete complex tasks. Fig. 11a shows the motion ability of the “Humanoid” robot in the “Gaps” task environment. Driven by the NIHRL algorithm, the robot exhibits jumping behavior that allows it to freely cross magma. From Fig. 11b, it can be seen that the “Walker” robot will naturally change its posture when encountering obstacles higher than its own body. Fig. 11c shows the target tracking skill of the “Quadruped” robot in the “Goals” task. Fig. 11d shows the ability of the “Humanoid” robot to climb stairs. Fig. 11e depicts the hurdle-crossing ability evolved by the “Cheetah” robot in the “Hurdles” task. Finally, Fig. 11f shows the speed adjustment function of the “Walker” robot.

VI. CONCLUSION

Pre-training reinforcement learning has shown excellent performance in robot motion control. This article presents a novel NIHRL algorithm based on the structure of the central motor system. Our learning framework can enable robots to exhibit motion learning abilities similar to those of animals. Through pre-training, the cerebellar network can enable different types of robots to acquire basic motion regulation abilities. Through task-training, robots can quickly adapt to various downstream tasks. In addition, we propose a skill activity function based on the mechanism of the basal ganglia, which can enable robots to autonomously generate motor willingness. And a skill encoding method with skill diverse objective is proposed

to improve the independence between skills. We demonstrate the rationality of the algorithm components through theoretical analysis and experiments. Furthermore, compared to SOTA baselines, our algorithm demonstrate excellent performance in various robot and task environments. As for future works, combining NIHRL with CPG control methods [13] [14] based on spinal reflex mode is an interesting direction.

REFERENCES

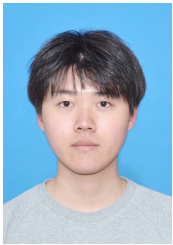
- [1] R. S. Sutton and A. G. Barto, *Reinforcement learning: An introduction*. MIT press, 2018.
- [2] J. Hwangbo, J. Lee, A. Dosovitskiy *et al.*, “Learning agile and dynamic motor skills for legged robots,” *Science Robotics*, vol. 4, no. 26, p. eaau5872, 2019.
- [3] N. Heess, D. Tb, S. Sriram *et al.*, “Emergence of locomotion behaviours in rich environments,” *arXiv preprint arXiv:1707.02286*, 2017.
- [4] R. Bommasani, D. A. Hudson, E. Adeli *et al.*, “On the opportunities and risks of foundation models,” *arXiv preprint arXiv:2108.07258*, 2021.
- [5] S. Pateria, B. Subagdja, A.-h. Tan *et al.*, “Hierarchical reinforcement learning: A comprehensive survey,” *ACM Computing Surveys (CSUR)*, vol. 54, no. 5, pp. 1–35, 2021.
- [6] M. Laskin, D. Yarats, H. Liu *et al.*, “Urb: Unsupervised reinforcement learning benchmark,” *arXiv preprint arXiv:2110.15191*, 2021.
- [7] J. Gehring, G. Synnaeve, A. Krause *et al.*, “Hierarchical skills for efficient exploration,” *Advances in Neural Information Processing Systems*, vol. 34, pp. 11 553–11 564, 2021.
- [8] X. B. Peng, Y. Guo, L. Halper *et al.*, “Ase: Large-scale reusable adversarial skill embeddings for physically simulated characters,” *ACM Transactions On Graphics (TOG)*, vol. 41, no. 4, pp. 1–17, 2022.
- [9] M. Bear, B. Connors, and M. A. Paradiso, *Neuroscience: exploring the brain, enhanced edition: exploring the brain*. Jones & Bartlett Learning, 2020.
- [10] E. V. Everts, “Brain mechanisms in movement,” *Scientific American*, vol. 229, no. 1, pp. 96–103, 1973.
- [11] P. J. Whelan, “Control of locomotion in the decerebrate cat,” *Progress in neurobiology*, vol. 49, no. 5, pp. 481–515, 1996.
- [12] R. David McK, “Certain aspects of the behavior of decorticate cats,” *Psychiatry*, vol. 1, no. 3, pp. 339–345, 1938.
- [13] E. Marder and D. Bucher, “Central pattern generators and the control of rhythmic movements,” *Current biology*, vol. 11, no. 23, pp. R986–R996, 2001.

TABLE IV
AVERAGE SCORE OF DIFFERENT METHODS IN DIFFERENT TASKS

Method		SAC	APS	No N-SD+No $h(z)R_e$	No $h(z)R_e$	No N-SD	NIHRL
Cheetah	Gaps	0.0 \pm 0.0	16.1 \pm 1.7	5.5 \pm 6.4	0.7 \pm 1.4	12.5 \pm 1.7	7.9 \pm 0.4
	Goals	27.5 \pm 18.6	11.5 \pm 3.2	3.1 \pm 1.3	3.9 \pm 2.6	13.8 \pm 1.6	10.9 \pm 0.5
	Stairs	9.9 \pm 11.4	18.8 \pm 0.6	18.8 \pm 0.9	19.0 \pm 1.0	19.7 \pm 0.1	19.5 \pm 0.3
	Hurdles	0.0 \pm 0.1	31.7 \pm 0.6	22.4 \pm 3.8	16.4 \pm 1.9	32.0 \pm 3.0	29.3 \pm 2.1
	V-track	964.6 \pm 10.3	345.5 \pm 145.7	352.5 \pm 49.6	276.2 \pm 32.7	718.9 \pm 68.5	568.0 \pm 73.0
Walker	Gaps	0.0 \pm 0.0	0.0 \pm 0.0	0.0 \pm 0.0	0.0 \pm 0.0	19.6 \pm 3.5	17.8 \pm 2.3
	Goals	0.0 \pm 0.0	0.0 \pm 0.0	0.0 \pm 0.0	0.0 \pm 0.0	10.1 \pm 1.5	9.3 \pm 0.5
	Stairs	16.5 \pm 1.9	0.1 \pm 0.2	16.9 \pm 0.9	0.3 \pm 0.3	17.0 \pm 0.8	13.9 \pm 1.9
	Hurdles	17.7 \pm 3.3	0.0 \pm 0.0	4.8 \pm 4.7	0.6 \pm 0.7	15.6 \pm 2.3	15.5 \pm 0.5
	V-track	877.5 \pm 16.0	255.5 \pm 53.4	324.1 \pm 36.5	145.6 \pm 196.5	796.4 \pm 6.5	790.3 \pm 24.3
	Limbos	5.3 \pm 7.0	0.0 \pm 0.0	0.0 \pm 0.0	0.0 \pm 0.0	5.3 \pm 2.7	9.0 \pm 2.5
Quadruped	Gaps	0.0 \pm 0.0	0.0 \pm 0.0	0.0 \pm 0.0	0.0 \pm 0.0	6.7 \pm 0.8	4.5 \pm 0.4
	Goals	0.0 \pm 0.0	0.0 \pm 0.0	0.0 \pm 0.0	0.0 \pm 0.0	17.1 \pm 0.4	13.6 \pm 0.3
	Stairs	0.0 \pm 0.0	0.0 \pm 0.0	0.0 \pm 0.0	0.0 \pm 0.0	16.7 \pm 0.6	14.3 \pm 2.5
	Hurdles	0.0 \pm 0.0	0.7 \pm 1.0	0.0 \pm 0.0	0.0 \pm 0.0	7.5 \pm 0.7	5.0 \pm 3.7
	V-track	359.7 \pm 98.2	53.5 \pm 24.6	55.2 \pm 9.0	79.1 \pm 32.1	214.7 \pm 48.8	294.3 \pm 132.9
Humanoid	Gaps	0.0 \pm 0.0	0.0 \pm 0.0	0.0 \pm 0.0	0.0 \pm 0.0	0.3 \pm 0.5	2.2 \pm 2.2
	Goals	0.0 \pm 0.0	0.0 \pm 0.0	0.0 \pm 0.0	0.0 \pm 0.0	6.1 \pm 1.7	5.4 \pm 0.9
	Stairs	0.0 \pm 0.0	0.0 \pm 0.0	0.0 \pm 0.0	0.2 \pm 0.4	5.8 \pm 3.2	7.9 \pm 1.1
	Hurdles	0.0 \pm 0.1	0.0 \pm 0.1	0.0 \pm 0.0	0.4 \pm 0.5	3.0 \pm 1.4	2.7 \pm 0.2
	V-track	455.7 \pm 113.4	95.3 \pm 14.3	161.9 \pm 19.1	169.1 \pm 91.2	487.3 \pm 55.4	342.3 \pm 64.6
	Limbos	0.2 \pm 0.4	0.0 \pm 0.0	0.0 \pm 0.0	0.0 \pm 0.0	1.8 \pm 0.9	3.0 \pm 1.0

- [14] A. J. Ijspeert, "Central pattern generators for locomotion control in animals and robots: a review," *Neural networks*, vol. 21, no. 4, pp. 642–653, 2008.
- [15] I. Bar-Gad, G. Morris, and H. Bergman, "Information processing, dimensionality reduction and reinforcement learning in the basal ganglia," *Progress in neurobiology*, vol. 71, no. 6, pp. 439–473, 2003.
- [16] A. M. Graybiel, "The basal ganglia," *Current biology*, vol. 10, no. 14, pp. R509–R511, 2000.
- [17] K. Doya, "Complementary roles of basal ganglia and cerebellum in learning and motor control," *Current opinion in neurobiology*, vol. 10, no. 6, pp. 732–739, 2000.
- [18] E. Hazan, S. Kakade, K. Singh *et al.*, "Provably efficient maximum entropy exploration," in *International Conference on Machine Learning*. PMLR, 2019, pp. 2681–2691.
- [19] H. Liu and P. Abbeel, "Behavior from the void: Unsupervised active pre-training," *Advances in Neural Information Processing Systems*, vol. 34, pp. 18 459–18 473, 2021.
- [20] D. Yarats, R. Fergus, A. Lazaric *et al.*, "Reinforcement learning with prototypical representations," in *International Conference on Machine Learning*. PMLR, 2021, pp. 11 920–11 931.
- [21] J. Achiam, H. Edwards, D. Amodei *et al.*, "Variational option discovery algorithms," *arXiv preprint arXiv:1807.10299*, 2018.
- [22] S. Park, J. Choi, J. Kim *et al.*, "Lipschitz-constrained unsupervised skill discovery," in *International Conference on Learning Representations*, 2021.
- [23] B. Eysenbach, A. Gupta, J. Ibarz *et al.*, "Diversity is all you need: Learning skills without a reward function," *arXiv preprint arXiv:1802.06070*, 2018.
- [24] H. Liu and P. Abbeel, "Aps: Active pretraining with successor features," in *International Conference on Machine Learning*. PMLR, 2021, pp. 6736–6747.
- [25] S. Hansen, W. Dabney, A. Barreto *et al.*, "Fast task inference with variational intrinsic successor features," *arXiv preprint arXiv:1906.05030*, 2019.
- [26] D. Pathak, P. Agrawal, A. A. Efros *et al.*, "Curiosity-driven exploration by self-supervised prediction," pp. 2778–2787, 2017.
- [27] Y. Burda, H. Edwards, A. Storkey *et al.*, "Exploration by random network distillation," *arXiv preprint arXiv:1810.12894*, 2018.
- [28] H. Shi, B. Zhou, H. Zeng *et al.*, "Reinforcement learning with evolutionary trajectory generator: A general approach for quadrupedal locomotion," *IEEE Robotics and Automation Letters*, vol. 7, no. 2, pp. 3085–3092, 2022.
- [29] V. Campos, A. Trott, C. Xiong *et al.*, "Explore, discover and learn: Unsupervised discovery of state-covering skills," in *International Conference on Machine Learning*. PMLR, 2020, pp. 1317–1327.
- [30] T. Kwon and J. K. Hodgins, "Momentum-mapped inverted pendulum models for controlling dynamic human motions," *ACM Transactions on Graphics (TOG)*, vol. 36, no. 1, pp. 1–14, 2017.
- [31] P. Xu and I. Karamouzas, "A gan-like approach for physics-based imitation learning and interactive character control," *Proceedings of the ACM on Computer Graphics and Interactive Techniques*, vol. 4, no. 3, pp. 1–22, 2021.
- [32] X. B. Peng, P. Abbeel, S. Levine *et al.*, "Deepmimic: Example-guided deep reinforcement learning of physics-based character skills," *ACM Transactions On Graphics (TOG)*, vol. 37, no. 4, pp. 1–14, 2018.
- [33] S. Park, H. Ryu, S. Lee *et al.*, "Learning predict-and-simulate policies from unorganized human motion data," *ACM Transactions on Graphics (TOG)*, vol. 38, no. 6, pp. 1–11, 2019.
- [34] X. B. Peng, G. Berseth, K. Yin *et al.*, "Deeploco: Dynamic locomotion skills using hierarchical deep reinforcement learning," *ACM Transactions on Graphics (TOG)*, vol. 36, no. 4, pp. 1–13, 2017.
- [35] W. J. Yun, M. Shin, D. Mohaisen *et al.*, "Hierarchical deep reinforcement learning-based propofol infusion assistant framework in anesthesia," *IEEE Transactions on Neural Networks and Learning Systems*, 2022.
- [36] K. Gregor, D. J. Rezende, and D. Wierstra, "Variational intrinsic control," *arXiv preprint arXiv:1611.07507*, 2016.
- [37] D. Barber and F. Agakov, "The im algorithm: a variational approach to information maximization," *Advances in neural information processing systems*, vol. 16, no. 320, p. 201, 2004.
- [38] K. Amunts, "Brodmann areas," *Encyclopedia of Evolutionary Psychological Science*, pp. 821–824, 2021.
- [39] M. Weinrich and S. P. Wise, "The premotor cortex of the monkey," *Journal of Neuroscience*, vol. 2, no. 9, pp. 1329–1345, 1982.
- [40] J. Phillips, J. Bradshaw, R. Iansel *et al.*, "Motor functions of the basal ganglia," *Psychological research*, vol. 55, pp. 175–181, 1993.
- [41] J. E. Visser and B. R. Bloem, "Role of the basal ganglia in balance control," *Neural plasticity*, vol. 12, no. 2–3, pp. 161–174, 2005.
- [42] A. Klaus, J. Alves da Silva, and R. M. Costa, "What, if, and when to move: basal ganglia circuits and self-paced action initiation," *Annual review of neuroscience*, vol. 42, pp. 459–483, 2019.

- [43] A. V. Kravitz, B. S. Freeze, P. R. Parker *et al.*, “Regulation of parkinsonian motor behaviours by optogenetic control of basal ganglia circuitry,” *Nature*, vol. 466, no. 7306, pp. 622–626, 2010.
- [44] E. Todorov, T. Erez, and Y. Tassa, “Mujoco: A physics engine for model-based control,” in *2012 IEEE/RSJ international conference on intelligent robots and systems*. IEEE, 2012, pp. 5026–5033.
- [45] T. Haarnoja, A. Zhou, K. Hartikainen *et al.*, “Soft actor-critic algorithms and applications,” *arXiv preprint arXiv:1812.05905*, 2018.
- [46] W. Whitney, R. Agarwal, K. Cho *et al.*, “Dynamics-aware embeddings,” *arXiv preprint arXiv:1908.09357*, 2019.
- [47] P. Dobrowolski, “Swing-twist decomposition in clifford algebra,” *arXiv preprint arXiv:1506.05481*, 2015.
- [48] L. Van der Maaten and G. Hinton, “Visualizing data using t-sne,” *Journal of machine learning research*, vol. 9, no. 11, 2008.
- [49] J. P. G. Vonsattel and M. DiFiglia, “Huntington disease,” *Journal of neuropathology and experimental neurology*, vol. 57, no. 5, p. 369, 1998.
- [50] W. Poewe and others, “Parkinson disease,” *Nature reviews Disease primers*, vol. 3, no. 1, pp. 1–21, 2017.



Pei Zhang received the B.Eng. degree from Northeastern University, Shenyang, Liaoning, China, in 2021. He is currently working toward the Ph.D. degree at the State Key Laboratory of Synthetical Automation for Process Industries, Northeastern University, Shenyang, Liaoning, China. His research interests include reinforcement learning, machine learning, and robotics.



Zhaobo Hua received the B.Eng. degree from Northeastern University, Shenyang, Liaoning, China, in 2023. He is currently working toward the Ph.D. degree at the State Key Laboratory of Synthetical Automation for Process Industries, Northeastern University, Shenyang, Liaoning, China. His research interests include reinforcement learning, machine learning, and robotics.



Jinliang Ding (Senior Member, IEEE) received the bachelor's, master's, and Ph.D. degrees in control theory and control engineering from Northeastern University, Shenyang, China, in 2001, 2004, and 2012, respectively.

He is currently a Professor with the State Key Laboratory of Synthetical Automation for Process Industry, Northeastern University. He has authored or coauthored over 100 refereed journal articles and refereed papers at international conferences. He has also invented or co-invented 20 patents. His current research interests include modeling, plant-wide control, optimization for complex industrial systems, stochastic distribution control, and multiobjective evolutionary algorithms and their applications.

Dr. Ding was a recipient of the three First-Prize of Science and Technology Awards of the Ministry of Education in 2006, 2012, and 2018, the International Federation of Automatic Control (IFAC) Control Engineering Practice for 2011–2013 Paper Prize, the National Technological Invention Award in 2013, the National Science Fund for Distinguished Young Scholars in 2015, and the Young Scholars Science and Technology Award of China in 2016. One of his articles published on control engineering practice was selected for the Best Paper Award from 2011 to 2013.